

Pigs are highly susceptible to but do not transmit mink-derived highly pathogenic avian influenza virus H5N1 clade 2.3.4.4b

Taeyong Kwon^a, Jessie D. Trujillo^a, Mariano Carossino^b, Eu Lim Lyoo^a, Chester D. McDowell^a, Konner Cool^a, Franco S. Matias-Ferreira^a, Trushar Jeevan^c, Igor Morozov^a, Natasha N. Gaudreault^a, Udeni B.R. Balasuriya^b, Richard J. Webby^c, Nikolaus Osterrieder^{a*} and Juergen A. Richt^a

^aDepartment of Diagnostic Medicine/Pathobiology, College of Veterinary Medicine, Kansas State University, Manhattan, KS, USA;

^bLouisiana Animal Disease Diagnostic Laboratory and Department of Pathobiological Sciences, School of Veterinary Medicine, Louisiana State University, Baton Rouge, LA, USA; ^cDepartment of Infectious Diseases, St. Jude Children's Research Hospital, Memphis, TN, USA

ABSTRACT

Rapid evolution of highly pathogenic avian influenza viruses (HPAIVs) is driven by antigenic drift but also by reassortment, which might result in robust replication in and transmission to mammals. Recently, spillover of clade 2.3.4.4b HPAIV to mammals including humans, and their transmission between mammalian species has been reported. This study aimed to evaluate the pathogenicity and transmissibility of a mink-derived clade 2.3.4.4b H5N1 HPAIV isolate from Spain in pigs. Experimental infection caused interstitial pneumonia with necrotizing bronchiolitis with high titers of virus present in the lower respiratory tract and 100% seroconversion. Infected pigs shed limited amount of virus, and importantly, there was no transmission to contact pigs. Notably, critical mammalian-like adaptations such as PB2-E627 K and HA-Q222L emerged at low frequencies in principal-infected pigs. It is concluded that pigs are highly susceptible to infection with the mink-derived clade 2.3.4.4b H5N1 HPAIV and provide a favorable environment for HPAIV to acquire mammalian-like adaptations.

ARTICLE HISTORY Received 8 January 2024; Revised 15 April 2024; Accepted 3 May 2024

KEYWORDS Pigs; clade 2.3.4.4b; highly pathogenic avian influenza virus; H5N1; mammalian-like adaptations, mink isolate, transmission

Introduction


Influenza A viruses (IAV) are members of the *Orthomyxoviridae* family and are single-stranded, negative-sense, segmented RNA viruses. IAVs are classified into different subtypes based on the two major surface proteins: hemagglutinin (HA) and neuraminidase (NA). Wild aquatic birds are natural hosts for most IAV subtypes, except for H17N10 and H18N11, which were first isolated from bats and seem endemic in multiple bat species [1,2]. Highly pathogenic avian influenza (HPAI) viruses arise from low pathogenic avian influenza (LPAI) viruses by insertion of a stretch of basic amino acids into the HA cleavage site, which enables efficient HA activation by ubiquitous cellular, furin-like proteases; they cause systemic, lethal infections in poultry [3].

Since the first detection of HPAI H5 subtype viruses with the isolation of the A/Goose/Guangdong/1/1996 (GsGD) H5N1 virus in southern China in 1996, this lineage has genetically evolved and spread worldwide primarily by migratory birds [4]. Continuous evolution of the GsGD-like H5 HPAI viruses lead

to the emergence of genetically distinct clades, and reassortment with other clades of HPAI viruses or local LPAI viruses has resulted in remarkable genetic diversification through the acquisition of novel gene segments [5]. Eventually, HPAI H5N1 clade 2 viruses became dominant and their descendants have been responsible for subsequent HPAI outbreaks. One remarkable HPAI outbreak in North America happened in 2014/2015, when Asian-origin HPAI H5 clade 2.3.4.4 viruses spread to North America via the Pacific flyway (Alaska, Western Canada/USA) with migratory wild birds and underwent reassortment with local North American LPAIVs, resulting in HPAI H5 viruses with multiple NA subtypes, including H5N1, H5N2, H5N5, H5N6, and H5N8, collectively called H5Nx viruses [6]. The geographic expansion of the H5Nx HPAI viruses via wild birds and increased molecular evolution resulted in the emergence and dominance of H5 subtype clade 2.3.4.4b viruses which contributed to the H5N8 outbreaks in 2016/17 and 2020/21 and the H5N1 outbreaks in 2021/22 [7]. By 2021/22, H5N1 clade

CONTACT Juergen A. Richt  jricht@ksu.edu

*Present address: Freie Universität Berlin, Institut für Virologie, Berlin, Germany.

 Supplemental data for this article can be accessed online at <https://doi.org/10.1080/22221751.2024.2353292>.

© 2024 The Author(s). Published by Informa UK Limited, trading as Taylor & Francis Group, on behalf of Shanghai Shangyixun Cultural Communication Co., Ltd. This is an Open Access article distributed under the terms of the Creative Commons Attribution-NonCommercial License (<http://creativecommons.org/licenses/by-nc/4.0/>), which permits unrestricted non-commercial use, distribution, and reproduction in any medium, provided the original work is properly cited. The terms on which this article has been published allow the posting of the Accepted Manuscript in a repository by the author(s) or with their consent.

2.3.4.4b infections had caused massive HPAI outbreaks in Europe with subsequent spread to North America via Iceland and the trans-Atlantic flyways [8].

The normal distribution of the receptors for avian and mammalian IAVs in the human respiratory tract usually prevents efficient direct transmission of avian IAVs to humans, since the respective avian-like receptor (sialic acid linked to galactose by an alpha-2,3 linkage) is found only on cells in the lower respiratory tract [9]. Nonetheless, in certain instances, the human-animal interface allows IAVs to cross species barriers and infect humans. Human infection with avian IAVs occurs sporadically and results in mild to severe illness with a wide range of clinical symptoms. Specifically, it has been reported that human infections with avian H5 and H7 subtype viruses can cause severe illness in humans with case fatality rates of 52% and 39%, respectively [10]. Importantly, the current epidemiological data do not provide evidence for sustained human-to-human transmission of HPAI H5 viruses [11]. Since the beginning of 2020, human infections with clade 2.3.4.4b H5N1 have been documented in China, Spain, UK, USA, and Vietnam, and all cases were linked to close contact with infected poultry [12]. In addition, the ability of the clade 2.3.4.4b H5N1 viruses to cross the species barrier is clearly supported by its detection in a variety of mammalian species such as terrestrial and marine mammals [12]. In October 2022, an outbreak of the clade 2.3.4.4b H5N1 HPAI virus in farmed mink in Spain was reported, with clear evidence of sustained mink-to-mink transmission [13], raising concerns about the adaptation of the clade 2.3.4.4b H5N1 virus to mammals. Therefore, in order to determine the risk of the mink-derived clade 2.3.4.4b H5N1 virus isolate, this study evaluated its virulence and transmissibility in pigs, which are natural hosts for IAVs and the “mixing vessel” for the reassortment and establishment of potentially pandemic influenza viruses.

Materials and methods

Cells and virus

Madin-Darby canine kidney (MDCK) cells were maintained in Dulbecco’s Modified Eagle Medium (DMEM; Corning, Manassas, VA, USA) supplemented with 5% fetal bovine serum (FBS; R&D systems, Flower Branch, GA, USA) and a 1% antibiotic-antimycotic solution (Gibco, Grand Island, NY, USA). The mink-derived clade 2.3.4.4b H5N1 isolate, A/Mink/Spain/3691-8_22VIR10586-10/2022, was kindly provided by Francesco Bonfante and Isabella Monne from the Istituto Zooprofilattico Sperimentale delle Venezie, Legnaro, Italy, and Monserrat Agüero and Azucena Sánchez from the Laboratorio Central

Veterinario (LCV), Ministry of Agriculture, Fisheries and Food, Madrid, Spain, via Dr. Richard Webby from St. Jude Children’s Research Hospital, Memphis, TN.

Pig infection experiment

All animal studies and experiments were approved and performed under the Kansas State University (KSU) Institutional Biosafety Committee (IBC, Protocol #1545) and the Institutional Animal Care and Use Committee (IACUC, Protocol #4778) in compliance with the Animal Welfare Act. All animal and laboratory work were performed in a biosafety level-3+ laboratory and ABSL-3Ag facility in the Biosecurity Research Institute at KSU in Manhattan, KS, USA. Fifteen 4-week-old piglets were obtained from a high health status pig herd at Kansas State University. The pigs were randomly separated into two groups: a principal-infected group and a sentinel group that were housed in separate pens. The number of animals used for this study was based on the animal holding capacity of the BSL-3Ag facility. Nine pigs were challenged with a total dose of 2.2×10^7 TCID₅₀ in 4 mL of DMEM: 1 mL orally, 1 mL intranasally, and 2 mL intratracheally (Figure 1(A)). On day 2 after infection, principal-infected and sentinel pigs were co-mingled and co-housed in a single pen. Nasal swab samples were collected in 2 mL of DMEM containing antibiotic/antimycotic solution at -1, 1 to 14, 17, and 21 days post-challenge (DPC), oropharyngeal swabs on days -1, 1, 3, 5, 7, 10, 14, 17, and 21 DPC. All pigs in this study were humanely euthanized by pentobarbital overdose and necropsied on planned days. The pigs were randomly selected for necropsy at 3 and 5 DPC since they did not develop severe clinical symptoms that met euthanasia criteria: three principal pigs at 3 DPC, three principal pigs at 5 DPC and the remaining 3 principal and 6 sentinel pigs at 21 DPC. At necropsy, gross pathology evaluation was performed and bronchoalveolar lavage fluid (BALF) and tissue samples were collected.

Virus isolation

All nasal swabs, oropharyngeal swabs, BALF and tissues samples were subjected to virus titration. Briefly, MDCK cells were used to titrate the virus from clinical samples, which were filtered through a 0.45 µm syringe filter except for BALF. Ten-fold serial dilutions of samples were prepared and transferred on confluent MDCK cells after washing with PBS. The plates were subjected to an immunofluorescence assay (IFA) on day 2. Briefly, the cells were fixed with ice-cold methanol and incubated with the HB65 monoclonal antibody targeting the IAV

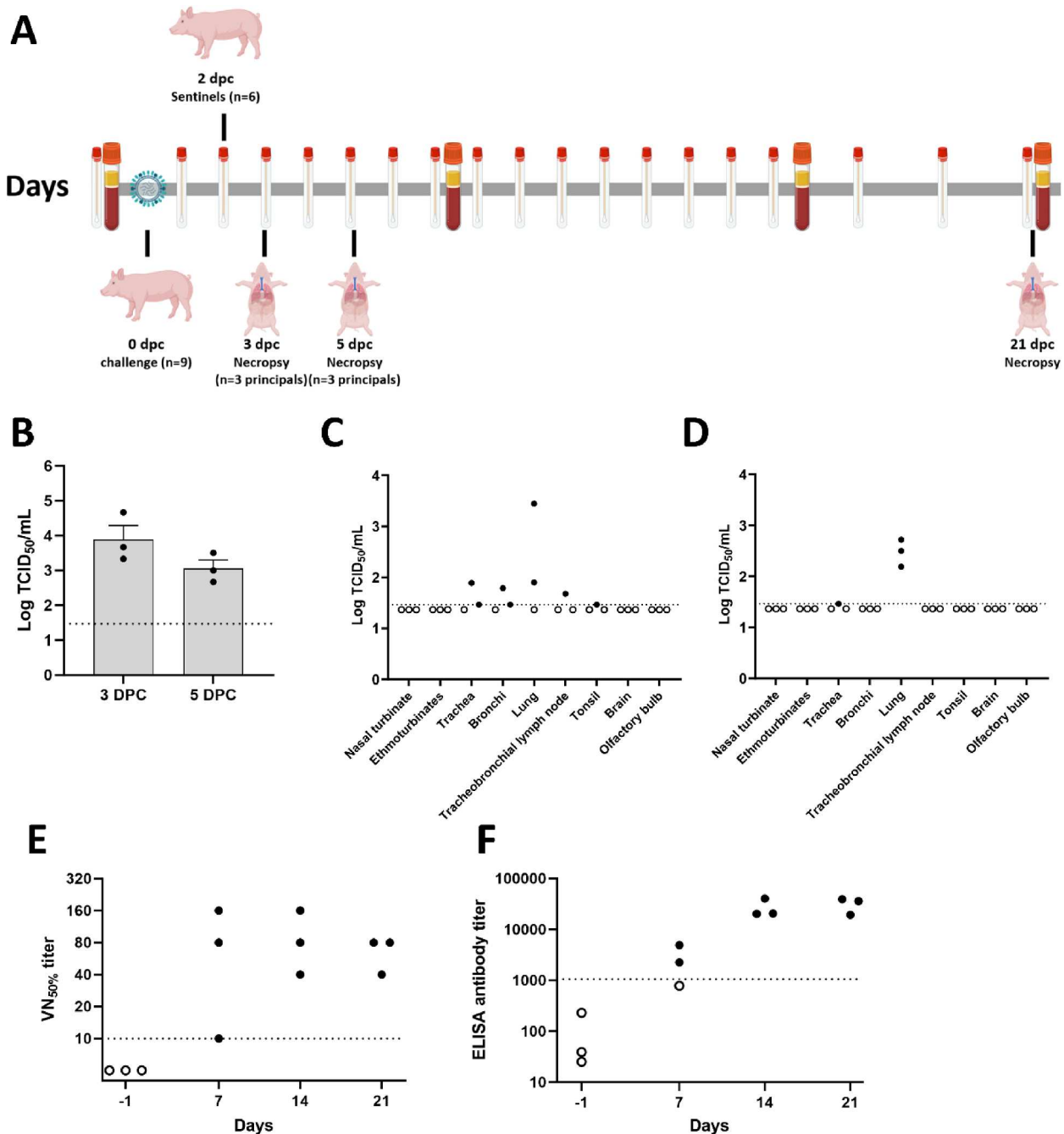


Figure 1. Infection with a mink-derived clade 2.3.4.4b H5N1 isolate in pigs. **A** The pigs ($n = 9$) were orally, intra-nasally, and intra-tracheally infected with 2.2×10^7 TCID₅₀ of A/Mink/Spain/3691-8_22VIR10586-10/2022 and sentinel pigs ($n = 6$) were introduced into the same pen at 2 days post-challenge (DPC). Swab and serum samples were collected throughout the study. Principal infected pigs were euthanized and necropsied at 3 and 5 DPC ($n = 3$ per time point) and the remaining three principals and 6 sentinels were euthanized and necropsied at 21 DPC. **B** Infectious virus titers in bronchoalveolar lavage fluids at 3 and 5 DPC and **C and D** infectious virus titers in tissues at (C) 3 DPC and (D) 5 DPC. **E and F** Antibody responses were evaluated in three principal pigs at -1 , 7, 14, and 21 DPC. Virus neutralization (VN) titers (E) were a reciprocal of the highest serum dilution inhibiting replication of the homologous H5N1 virus. ELISA antibody titers were determined using a porcine indirect ELISA kit (ID Screen® Influenza A Nucleoprotein Swine Indirect, Innovative Diagnostics, France) where S/P ratios were calculated from O.D. values and then converted to antibody titers according to the manufacturers' instruction. Dash lines represent the limit of detection of each assay (4.64×10^1 TCID₅₀/mL for BALF titration, 2.92×10^1 TCID₅₀/mL for tissue titration, 1:10 for VN assay, and 1053 for ELISA antibody titer). Empty circle represents negative results in each assay.

nucleoprotein [14]. After washing, the cells were incubated with anti-mouse antibodies conjugated with Alexa Fluor 488 (Invitrogen, Carlsbad, CA, USA). Virus titers were calculated using the Reed-Muench method [15]. The limit of detection was 46 TCID₅₀/mL.

RNA extraction and M gene-specific RT-qPCR

To determine viral RNA shedding and viral RNA distribution, viral RNA was extracted from all samples mentioned above using a magnetic bead-based automated extraction system (Taco Mini and total nucleic acid

extraction kit, Gene Reach, USA) [16]. Briefly, the swabs, BALF samples and 10% tissue homogenates were mixed with an equal volume of the RLT buffer (Qiagen, Germantown, MD, USA). Two hundred microliter of the sample lysate and 200 μ L isopropanol was added into the extraction plate. RT-qPCR was performed using the previously published primers and the modified probe (A to G at 66) in qScript XLT 1-Step RT-qPCR ToughMix (QuantaBio, Beverly, MA, USA) [17].

Serology

Virus neutralization tests were performed according to a previously established protocol [18]. Briefly, equal volumes of heat-treated serum (50 μ L) and 100 TCID₅₀/50 μ L of virus were mixed and incubated at 37°C for 1 h. The mixture was transferred onto pre-washed MDCK cells. On day 2, IFA was performed to determine 50% inhibition of virus growth. In addition, commercially available enzyme-linked immunosorbent assay (ELISA) kits were utilized according to the manufacturers' instruction: (1) ID Screen® Influenza A Nucleoprotein Swine Indirect, Innovative Diagnostics, France, (2) ID Screen® Influenza A Antibody Competition Multi-Species, Innovative Diagnostics, France, and (3) IDEXX AI MultiS-Screen Ab Test, IDEXX, USA.

Gross pathology and histopathology

Post-mortem examinations were conducted at 3, 5, and 21 DPC. Macroscopic pathology was scored *in toto*, and the percentage of lung lesions calculated based on the previous published protocols [19]. Tissue samples were fixed in 10% neutral buffered formalin, processed, and stained with hematoxylin and eosin (H&E). Microscopic pathology was evaluated based on microanatomy of the lung using a previously described scoring scale with minor modifications [20]. Each lung section was scored from 0 to 4 (0 = absent, 1 = minimal, 2 = mild, 3 = moderate, and 4 = severe) for six separate criteria typically associated with influenza A virus infections in pigs: (i) epithelial necrosis, attenuation or disruption; (ii) airway exudate; (iii) percentage of airways with inflammation; (iv) peribronchiolar and perivascular lymphocytic inflammation; (v) alveolar exudate; (vi) alveolar septal inflammation. For scoring the percentage of airways with inflammation (iii): 0% = 0, up to 10% involvement = 1, 10–39% involvement = 2, 40–69% involvement = 3 and, greater than 70% involvement = 4.

Influenza A virus-specific immunohistochemistry (IHC)

Immunohistochemistry (IHC) for detection of Influenza virus A H5N1 nucleoprotein (NP) antigen

was performed on the automated BOND RXm platform and the Polymer Refine Red Detection kit (Leica Biosystems, Buffalo Grove, IL). Following automated deparaffinization, four-micron formalin-fixed, paraffin-embedded tissue sections on positively charged Superfrost® Plus slides (VWR, Radnor, PA) were subjected to automated heat-induced epitope retrieval (HIER) using a ready-to-use EDTA-based retrieval solution (pH 9.0, Leica Biosystems) at 100°C for 20 min. Subsequently, tissue sections were incubated with the primary antibody (rabbit polyclonal anti-Influenza A virus NP [ThermoFisher Scientific, PA5-32242] diluted 1:500 in Primary Antibody diluent [Leica Biosystems]) for 30 min at ambient temperature followed by a polymer-labeled goat anti-rabbit IgG coupled with alkaline phosphatase (30 min). Fast Red was used as the chromogen (15 min), and counterstaining was performed with hematoxylin for 5 min. Slides were dried in a 60°C oven for 30 min and mounted with a permanent mounting medium (Micromount®, Leica Biosystems). Lung sections from a pig experimentally infected with swine influenza virus A/swine/Texas/4199-2/1998 H3N2 were used as a positive assay control.

Influenza A virus H5N1 mink-specific RNAscope® in situ hybridization

For RNAscope® in situ hybridization (ISH), an anti-sense probe targeting the NP and the hemagglutinin (HA [H5 subtype]) of influenza virus A/Mink/Spain/3691-8_22VIR10586-10/2022 clade 2.3.4.4b (GISAID # EPI_ISL_15878539) were designed (Advanced Cell Diagnostics (ACD), Newark, CA, USA). Sections of formalin-fixed paraffin-embedded tissues were generated as indicated above, and the RNAscope® ISH assay was performed using the RNAscope 2.5 LSx Reagent Kit (ACD) on the automated BOND RXm platform (Leica Biosystems, Buffalo Grove, IL, USA). Following automated baking and deparaffinization, tissue sections were subjected to heat-induced epitope retrieval (HIER) using an EDTA-based solution (pH 9.0; Leica Biosystems) at 100°C for 15 min, protease digestion using the RNAscope® 2.5 LSx Protease for 15 min at 40 °C, and incubation with a ready-to-use hydrogen peroxide solution for 10 min at room temperature. Slides were incubated with each probe mixture for 2 h at 40 °C, and the signal was amplified using a specific set of amplifiers (AMP1 through AMP6) as recommended by the manufacturer. The signal was detected using a Fast-Red solution for 10 min at room temperature. Slides were counterstained with a ready-to-use hematoxylin for 5 min, followed by five washes with 1X BOND Wash Solution (Leica Biosystems). Slides were finally rinsed in deionized water, dried in a 60 °C oven for 30 min, and mounted with Ecomount® (Biocare, Concord, CA, USA). Lung

sections from a pig experimentally infected with swine influenza virus A/swine/Texas/4199-2/1998 H3N2 were used as a positive assay control for the NP-specific probe, while lung sections from this study were used in conjunction with the former to validate the HA-specific probe.

Next-generation sequencing (NGS)

The whole genome sequence of the mink-derived H5N1 clade 2.3.4.4b virus was determined using the Illumina MiSeq sequencing platform (Illumina, San Diego, CA, USA). Briefly, viral RNA was extracted from the challenge virus inoculum and virus-positive clinical samples using the QIAamp viral RNA mini kit (Qiagen, Germantown, MD, USA) according to the manufacturer's instructions. Viral gene segments were amplified using SuperScript™ III One-Step RT-PCR System with Platinum™ Taq DNA Polymerase (Thermo Fisher Scientific, Waltham, WA, USA) with the Opti and Uni universal influenza primer sets [21,22] or with SuperScript™ IV First-Strand Synthesis System and Platinum™ SuperFi™ DNA Polymerase (Thermo Fisher Scientific, Waltham, WA, USA) with previously published segment specific primer sets [23]. Sequencing libraries were prepared using the Illumina DNA Prep kit (Illumina, San Diego, CA) and sequenced using the Illumina MiSeq platform with the Miseq v2 Reagent kit (300 cycles). Reads were demultiplexed and parsed into individual FASTQ files and imported into CLC Genomics Workbench version 22.0.1 (Qiagen, Germantown, MD, USA) for analysis. The trimmed reads were mapped to the reference sequences (GISAID accession numbers: EPI2220590 to EPI2220597). Following read mapping, all samples were run through the low frequency variant caller module within CLC Genomic Workbench with a frequency cutoff greater than 2%.

Results

Infection of pigs with the mink-derived clade 2.3.4.4b H5N1

This study aimed to elucidate the pathogenicity and transmissibility of the mink-derived clade 2.3.4.4b H5N1 virus in pigs. At 24 hours post-challenge, all

principal-infected pigs became lethargic, and five of nine pigs were febrile with average temperatures of 41°C. However, the average temperature decreased to 39.5°C at 2 DPC and pigs were healthy with no obvious clinical signs throughout the rest of the observation period (Supplementary Figure 1).

Infectious virus was isolated from nasal (6/9 animals positive) and oropharyngeal swabs (4/9 positive) from principal infected pigs and the titers ranged from 4.46×10^1 to 1×10^3 TCID₅₀/mL at 1 DPC (Table 1). At 3 DPC, one nasal and one oropharyngeal swab were virus positive, with titers of 2.15×10^3 and 4.64×10^2 TCID₅₀/mL, respectively. Infectious virus was still present in the nasal swabs at 5 DPC (2.15×10^2 TCID₅₀/mL). RT-qPCR results showed that all principal-infected animals were positive on at least one time point from 1 to 5 DPC in either the nasal or oropharyngeal swabs (Supplementary Figure 2(A, B)). All swabs collected from sentinel pigs were negative by virus isolation and RT-qPCR throughout the entire observation period.

To determine virus replication and distribution in tissues, virus titers were determined in BALF and various tissue samples. All BALF samples at 3 and 5 DPC were positive with titers of 2.15×10^3 – 4.64×10^4 TCID₅₀/mL at 3 DPC and 4.64×10^2 – 3.16×10^3 TCID₅₀/mL at 5 DPC (Figure 1(B)). Infectious virus could also be isolated from tracheas (3/6), bronchi (2/6), lung tissues (5/6), tracheobronchial lymph nodes (1/6), and tonsils (1/6) of the six principal-infected pigs that were euthanized at 3 ($n = 3$ pigs) and 5 ($n = 3$ pigs) DPC (Figure 1(C,D)). Interestingly, viral RNA was detectable in the ethmoturbinates of all three animals sacrificed at 3 DPC (Supplementary Figure 2(C)). In addition, viral RNA was present in the nasal turbinate of one pig at 3 DPC; this pig shed infectious virus from the nasal cavity at 1 and 3 DPC. In contrast, the brain and olfactory bulb at 3 and 5 DPC were negative as assessed by virus isolation and RT-qPCR (Supplementary Figure 2(C,D)). As expected, BALF and tissue samples from principal-infected and sentinel animals at 21 DPC were negative by both virus isolation and RT-qPCR.

Neutralizing antibodies were detectable in all three principal-infected animals starting at 7 DPC and all principals were sero-positive at 14 and 21 DPC (Figure 1(E)), with neutralization titers ranging from

Table 1. Virus shedding in pigs infected with the mink-derived clade 2.3.4.4b H5N1 virus.

Days post-challenge (DPC)			1	2	3	4	5	6 to 21 ^a
Nasal swab	Principal	# of positive / # of animals	6/9	0/9	1/9	0/6	1/6	0/3
		Virus titer (TCID ₅₀ /mL)	4.6×10^1 to 1×10^3	Neg	2.15×10^3	Neg	2.15×10^2	Neg
Oropharyngeal swab	Sentinel	# of positive / # of animals	0/6	0/6	0/6	0/6	0/6	0/6
	Principal	# of positive / # of animals	4/9	N/A ^b	1/9	N/A ^b	0/6	0/3
		Virus titer (TCID ₅₀ /mL)	1×10^2 to 4.6×10^2	N/A ^b	4.6×10^2	N/A ^b	Neg	Neg
	Sentinel	# of positive / # of animals	0/6	N/A ^b	0/6	N/A ^b	0/6	0/6

^aNasal swabs were collected at 6 to 14, 17 and 21 DPC and oropharyngeal swabs were at 7, 10, 14, 17, and 21 DPC.

^bN/A: Samples were not collected.

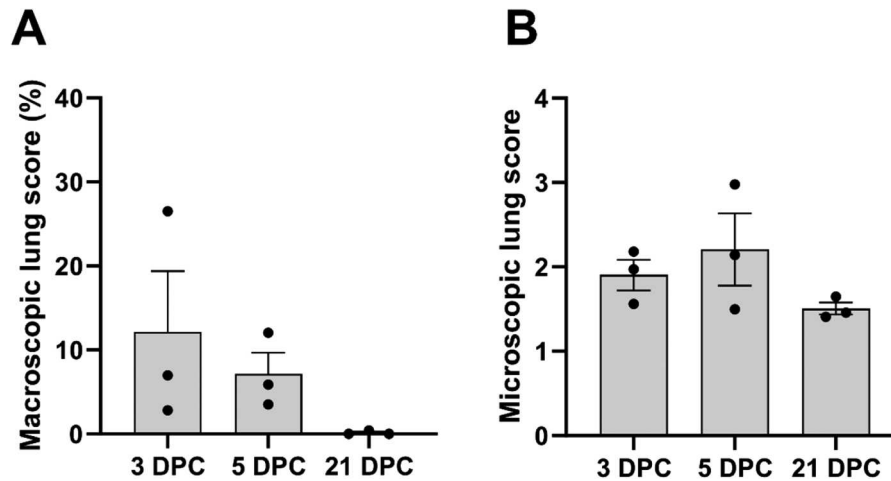


Figure 2. Macroscopic and microscopic lung scores in mink-derived clade 2.3.4.4b H5N1 virus-infected pigs. Infected pigs were euthanized at 3, 5, and 21 DPC for pathological evaluation. Macroscopic lung scores were determined by the percentage of the surface area showing IAV-induced pneumonia. Microscopic scores were calculated by the average of six different criteria (see Materials and Methods)

1:10 to 1:160. The NP-based indirect ELISA revealed that two out of three principal-infected animals seroconverted at 7 DPC, with the levels of antibodies in all three principal-infected pigs against NP increasing by 14 and 21 DPC (Figure 1(F)). Two different NP-based competitive ELISAs confirmed the seroconversion of the three principal-infected pigs at 14 and 21 DPC (Supplementary Figure 3(A,B)).

Macroscopic and microscopic pathology

At 3 DPC, moderate to severe, multifocal to coalescing interstitial pneumonia with marked congestion and edema affecting all lobes were noted in 2/3 euthanized animals, while the remaining animal had mild, multifocal pneumonia with congestion predominately on the right lung and left caudal lung lobes (Figure 2 and Supplementary Figure 4(A–C)). Pulmonary lesions consisted of moderate to severe non-suppurative interstitial pneumonia with necrotizing bronchitis/bronchiolitis affecting multiple bronchopulmonary segments, predominantly the pulmonary parenchyma adjacent to terminal bronchioles. Affected bronchopulmonary segments were characterized by degeneration, attenuation and necrosis of the bronchiolar epithelium and intraluminal cell debris and degenerate neutrophils, as well as peribronchiolar and perivascular histiocytic, neutrophilic and lymphocytic inflammation, locally extending to and expanding alveolar septa. Smaller bronchi and bronchioles were most commonly affected, and necrotizing alveolitis was characterized by alveolar spaces that contain inflammatory cells, occasional fibrin and necrotic cell debris; the epithelial lining was segmentally to partially denuded or lined by swollen degenerate epithelium (Figure 3(A)). These microscopic changes correlated with intracytoplasmic and/or intranuclear viral NP antigen frequently within

bronchial/bronchiolar epithelial cells, and less frequently within pneumocytes and alveolar macrophages (Figure 3(B)). Viral NP (as determined by NP-specific IHC) and H5-specific NP or HA RNA (as determined by RNAscope® ISH) were predominantly detected within airway epithelia and intraluminal necrotic cell debris, and sporadically in inflammatory cells within the bronchiolar lamina propria (Figure 4(A,B)). In 1/3 pigs (#839), there was localized suppurative and erosive rhinitis affecting the olfactory region (Supplementary Figure 5(A)). Within the affected region, viral antigen was detected in sporadic foci of the olfactory neuroepithelium (Supplementary Figure 5(B)). Larger airways (segmental bronchi and trachea) were affected by mild, multifocal neutrophilic to lymphohistiocytic bronchitis and tracheitis, with frequent bronchial but rare tracheal epithelial cells containing viral antigen (Supplementary Figure 5(C,D)).

By 5 DPC, multifocal to coalescing areas of pulmonary consolidation were observed on all pigs (Supplementary Figure 4(D–F)). Microscopically, alterations were similar to but more extensive than those at 3 DPC with intense inflammation affecting larger regions of the pulmonary parenchyma, with frequent bronchial/bronchiolar involvement and locally extensive alveolar collapse and consolidation (Figure 3(C)). Viral NP antigen and, less frequently, NP- and HA-specific RNA were detected in alveolar macrophages and intraluminal cell debris (Figures 3 and 4(C,D)). In addition, numerous individual and small clusters of epithelia on medium to large airways contained viral antigen. Microscopic changes in the trachea were mild and characterized by neutrophilic and lymphohistiocytic tracheitis with sporadic epithelial cell degeneration/necrosis and rare intracytoplasmic viral antigen (Supplementary Figure 5(E,F)). Multifocal, mild suppurative to erosive rhinitis

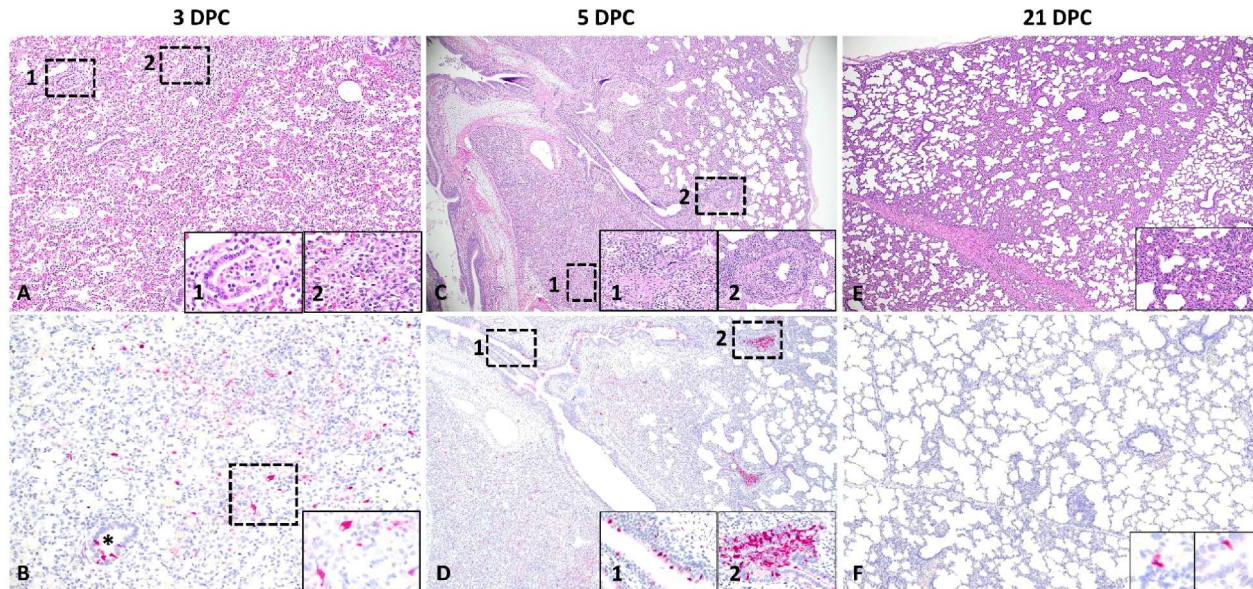


Figure 3. Histological features and tropism of mink-derived H5N1 clade 2.3.4.4b influenza virus in pigs. Histologically, pulmonary lesions were characterized by necrotizing to lymphohistiocytic bronchointerstitial pneumonia. At 3 DPC (A and B), multifocal broncho-pulmonary segments were characterized by bronchiolar epithelial cell necrosis (A, inset 1) and associated areas of pulmonary parenchyma with expanded alveolar septa infiltrated by lymphocytes and histiocytes and alveolar epithelial necrosis (A, inset 2). Influenza A virus NP intracytoplasmic antigen was detected within bronchiolar epithelial cells (B, asterisk), pneumocytes and alveolar macrophages (B, inset). Intranuclear viral antigen was typically detected within infected epithelial cells. Similar but more extensive and severe histological changes were noted at 5 DPC (C and D), with similar alveolar (C, inset 1) and bronchiolar (C, inset 2) alterations. Influenza A virus NP antigen was more abundant but had a similar cellular distribution compared to 3 DPC (D and insets 1 and 2). At 21 DPC, the airway epithelia had mostly repaired but multifocal areas of interstitial inflammation persisted (E, inset). Only sporadic epithelial cells contained viral antigen at this timepoint (F and insets). Magnifications of images: 12.5 \times for 3C and 3D, 20 \times for 3E, 40 \times for 3A and 3F, and 100 \times for 3B. Magnifications of insets: 40 \times for 3C and 3E, 200 \times for 3A and 3D, and 400 \times 3B and 3F.

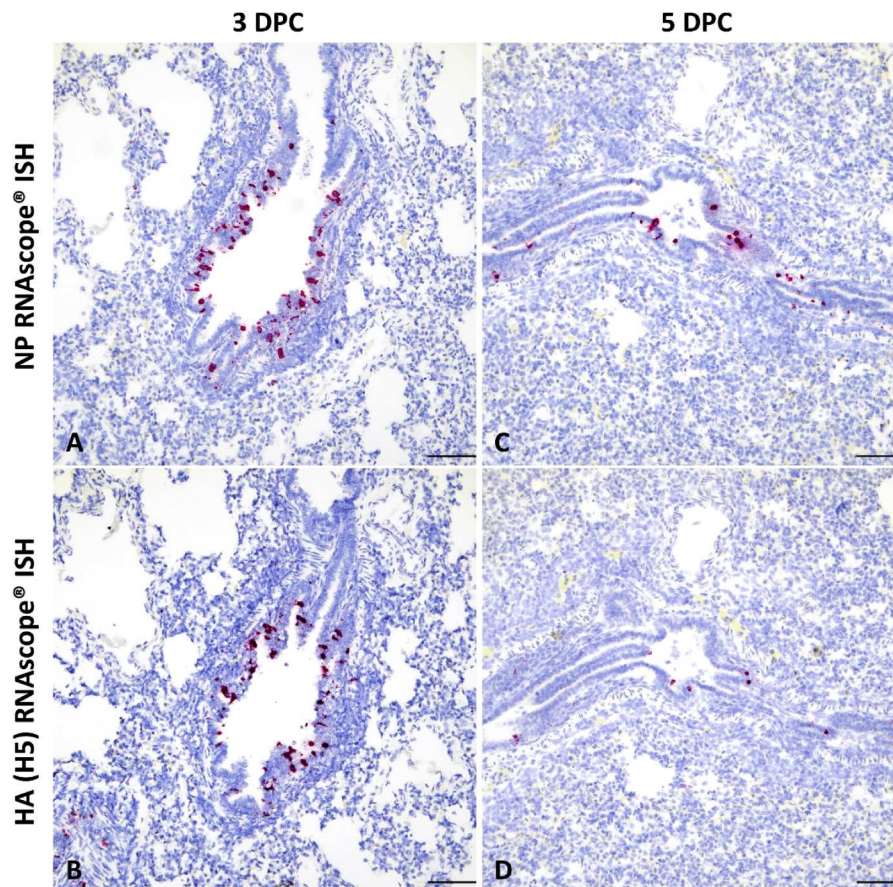


Figure 4. Detection of mink-derived H5N1 clade 2.3.4.4b influenza virus RNA via in situ hybridization (ISH). Probes specific to the NP and HA (H5) genes were designed. Viral RNA was predominantly detected within bronchiolar epithelial cells and intraluminal cellular debris at 3 (A and B) and 5 (C and D) DPC. RNAscope® ISH, Fast Red, total magnification 200 \times (the bar = 100 microns).

affecting rostral turbinates was identified, although in lieu of intralesional viral antigen. On 21 DPC, multiple foci of mild lymphohistiocytic interstitial pneumonia were noted, accompanied by bronchiolar epithelial hyperplasia (repair) with very rare bronchiolar epithelial cells or proprial mononuclear cells containing viral antigen (Figure 3(E,F)).

Interestingly, Influenza A virus NP-positive antigen presenting cells were common within tracheobronchial lymph nodes, most abundant at 3 DPC and gradually reducing in numbers through 21 DPC (Supplementary Figure 6). No other significant gross or histologic lesions, or viral antigen were identified in other organs examined.

Emergence of mammalian-like mutations in H5N1-infected pigs

The whole-length genome of the H5N1 virus inoculum, two nasal swabs, five oropharyngeal swabs and six BALF samples were genetically characterized to determine genetic evolution of the H5N1 virus after replication for up to 5 days in pigs. Our results show that the original mammalian-like PB2 T271A mutation present in the inoculum remained stable with a frequency below 2% with no evidence of a change in mutational frequency after virus replication for several days in pigs (Table 2 and Supplementary Table 1). Amino acid substitutions with a significant frequency (>2%) were found throughout all eight viral segments in clinical samples from H5N1-infected pigs; these mutations were below a frequency of 2% in the virus inoculum (Supplementary Table 1). NGS analysis revealed that oropharyngeal swab #517 on 1 DPC had the mammalian-like K526R mutation of PB2 at a frequency of approximately 3% (Table 2). Interestingly, the critical mammalian adaptation mutations, PB2-E627K and PB2-E627V, were identified in the oropharyngeal swab of pig #571 (E627K; 1 DPC), the BALF sample of pig #839 (E627K; 3 DPC), in the oropharyngeal swab of pig #94 (E627V; 1 DPC) and the BALF sample of pig #213 (E627V; 5 DPC) at a frequency of approximately 5%, 5%, 7% or 2%, respectively (Table 2). Furthermore, the oropharyngeal swab of pig #94 (1 DPC) had the Q222L substitution in the HA gene at the frequency of 2.1%. In individual animals, the sample containing the mammalian-like adaptation was collected at single time points.

Discussion

Molecular evolution allows IAVs to cross species barriers and to acquire the ability to infect a wide range of hosts from avian species to swine to humans and very recently even cattle. This broad host tropism provides opportunities for IAVs to gain distinct geno- and

Table 2. Mammalian-like adaptive mutations after replication of a mink-derived clade 2.3.4.4b H5N1 in pigs.

Viral protein	Amino acid substitution	Inoculum	Nasal swab, #517, 1 DPC		OP swab, #517, 1 DPC		OP swab, #571, 1 DPC		OP swab, #839, 1 DPC		OP swab, #634, 3 DPC		BALF, #517, 3 DPC		BALF, #571, 3 DPC		BALF, #839, 3 DPC		BALF, #94, 5 DPC		BALF, #213, 5 DPC		BALF, #714, 5 DPC	
			<2%	<2%	<2%	<2%	3.14%	<2%	<2%	<2%	<2%	<2%	<2%	<2%	<2%	<2%	<2%	<2%	<2%	<2%	<2%	<2%	<2%	<2%
PB2 ^a	K526R	<2%	<2%	<2%	3.14%	<2%	<2%	<2%	<2%	<2%	<2%	<2%	<2%	<2%	<2%	<2%	<2%	<2%	<2%	<2%	<2%	<2%	<2%	<2%
	E627K	<2%	<2%	<2%	<2%	4.71%	<2%	<2%	<2%	<2%	<2%	<2%	<2%	<2%	<2%	<2%	<2%	5.19%	<2%	<2%	<2%	<2%	<2%	<2%
	E627V	<2%	<2%	<2%	<2%	<2%	<2%	<2%	<2%	<2%	<2%	<2%	<2%	<2%	<2%	<2%	<2%	<2%	<2%	<2%	<2%	2.02%	<2%	<2%
HA	Q222L	<2%	<2%	<2%	<2%	2.10%	<2%	<2%	<2%	<2%	<2%	<2%	<2%	<2%	<2%	<2%	<2%	<2%	<2%	<2%	<2%	<2%	<2%	<2%

^aAmino acid substitution with a frequency >2% was not found at position of 271 of PB2 in all samples tested.

phenotypes, to evade pre-existing immunity in humans, and to attain pandemic potential [24]. Inter-species transmission of avian IAVs to mammals can lead to mammalian-like adaptations, which could result in efficient replication of avian IAVs in the respective mammalian host [25]. In addition, interspecies transmission contributes to the emergence of reassortant viruses, as has been demonstrated in pigs. The latter was clearly evident with the avian/swine reassortant H2N3 influenza A viruses isolated from diseased swine from two farms in the United States [26] and with the emergence of the pandemic H1N1 virus in 2009 [27]. Specific host-virus-environment characteristics determine the emergence of novel IAVs with pandemic potential. For pandemic preparedness, it is critical to assess the potential pandemic risk of newly emerged IAVs; the evaluation of certain virus characteristics is mainly done by *in vitro* and sometimes also *in vivo* experiments [28]. However, it is also essential to assess the pathogenesis and transmissibility of IAVs in target animal models. Pigs are natural hosts for IAVs, and it is known that certain IAVs can be efficiently transmitted between pigs. Importantly, interspecies transmissions between human and pigs and *vice versa* are not uncommon and are facilitated by an extensive human-pig interface in various agricultural settings [29]. Furthermore, pigs express receptors specific for both, mammalian and avian IAVs, providing opportunities for co-infections and the subsequent generation of novel reassortant influenza viruses [30]. Recently, interspecies transmission of clade 2.3.4.4b H5N1 virus to mink and sustained mink-to-mink transmission was reported in Spain, and the mink-derived virus was phylogenetically related to avian-origin viruses, posing a significant concern to public health [13]. Therefore, it was crucial to evaluate the pathogenicity and transmissibility of the recently emerged clade 2.3.4.4b H5N1 virus isolated from diseased mink in domestic pigs.

One of the key findings in this study was that experimental infection of pigs with the mink-derived clade 2.3.4.4b H5N1 virus resulted in productive virus replication and seroconversion in 100% of the principal-infected pigs. Virus titers in BALF samples of principal-infected animals reached $10^{3.3}$ to $10^{4.7}$ TCID₅₀/mL at 3 DPC and declined to $10^{2.7}$ to $10^{3.5}$ TCID₅₀/mL at 5 DPC. In addition, the virus was found in other respiratory tissues, such as trachea, bronchi, and lung, as well as lymphoid tissues, such as tracheo-bronchial lymph nodes and tonsils. Moreover, gross and histological evaluation of various tissues demonstrated that the infection caused acute multifocal to coalescing necrotizing broncho-interstitial pneumonia at 3 and 5 DPC, with residual mild interstitial pneumonia still present at 21 DPC. Based on the microscopic lesion distribution, virus titers and viral antigen/RNA tissue expression, it is clear that the

lesions and distribution of this mink-derived clade 2.3.4.4b H5N1 virus mostly involved the lower respiratory tract with only mild alterations on the upper respiratory tract. A previous study also demonstrated virus replication of avian-derived H5Nx clade 2.3.4.4 HPAI viruses from North America in the lower respiratory tract of pigs upon experimental infection [31]. In the previous study, infection of pigs with the avian-origin H5Nx clade 2.3.4.4 viruses, isolated in 2014 and 2015 in the US, led to viral RNA detection in 80–100% of the animals and successful virus isolation in 60–100% of the BALF samples at 3 and 5 DPC [31]. Consistent with virus detection in the majority of animals, 60–100% of infected animals seroconverted by 21 DPC [31]. In addition, in a very recent study, low susceptibility of pigs against experimental infection with an avian-derived H5N1 clade 2.3.4.4b virus, isolated from chickens in Germany in 2022, was reported [32]. This chicken H5N1 clade 2.3.4.4b isolate lacked any mammalian-like mutations. Nasal and alimentary exposure of pigs to this avian-derived H5N1 clade 2.3.4.4b virus only resulted in marginal virus replication and a low rate (1/8) of seroconversion without inducing any clinical signs or pathological changes, indicating a rather high resistance of pigs to infection with the avian-derived H5N1 clade 2.3.4.4b virus without mammalian-like adaptations [32]. Interestingly, neither infectious virus, viral RNA nor histopathological changes were present in tissues from the central nervous system (CNS) of principal-infected pigs in our study. In recent spillover events, wild mammals infected with the clade 2.3.4.4b H5N1 virus primarily exhibited neurological symptoms with histopathological changes in brain as well as viral RNA detection in CNS tissues [33–35]. Similarly, the mink infected with the H5N1 clade 2.3.4.4b virus used in this study also showed neurological manifestations, such as ataxia and tremors [13]. However, we could not observe any neurological clinical signs in principal-infected pigs, indicating that the pathogenicity of the H5N1 clade 2.3.4.4b viruses could vary in different mammalian host species.

Experimental infection of pigs with LPAI viruses without mammalian-like adaptations were also previously performed, but none of the experimental infections with LPAI H5 viruses resulted in a productive infection [36]. We conclude from our present study with the mink-derived clade 2.3.4.4b H5N1 HPAI virus, that this virus is not only able to efficiently infect mink, but also pigs. The mink-derived H5N1 clade 2.3.4.4b virus efficiently replicated in the lower respiratory tract of pigs inducing sizeable lung lesions; in addition, nasal and oral shedding was observed on early days after infection although less efficient than reported for swine-derived influenza viruses [26,37]. However, it is important to note that the mink-derived H5N1 clade 2.3.4.4b virus was unable to spread from

principal-infected to co-mingled in-contact sentinel animals; this was most likely due to the limited amount of virus shedding by the nasal and oral cavities in principal-infected pigs.

Earlier studies showed that experimental infection of pigs with avian-origin LPAI H5 subtype viruses isolated between 1980 and 2005 led to nasal shedding of infectious virus of up to $10^{5.5}$ egg infectious doses (EID)₅₀/mL and $10^{5.3}$ EID₅₀/100 mg [38,39]. In addition, it was shown that experimental infection of pigs with human and avian-origin HPAI H5N1 viruses isolated early (1997) and later (2004) in the emergence of the HPAI H5N1 virus resulted in the isolation of infectious virus in nasal swabs/nasal tracts over the course of infection, but no pig-to-pig transmission [40,41]. When pigs were infected with the index human H5N1 HPAIV strain (HK156-97) and an initial chicken H5N1 HPAIV isolate (CHK258-97) by the oral and nasal routes, both the human and chicken H5N1 viruses replicated well in the nasal tract of pigs, with the chicken isolate to higher titers than the human virus. Importantly, neither the human nor the chicken H5N1 virus transmitted to contact pigs in the same pen [40]. Similarly, experimental studies on the replication and transmissibility of 2004 avian H5N1 HPAI viruses associated with human infections in Vietnam to pigs revealed that all H5N1 viruses tested replicated in the swine respiratory tract but none were transmitted to contact pigs [39,41]. Epidemiological studies showed limited serologic evidence (8/3175 pigs positive) of exposure to the HPAI H5N1 viruses in Vietnamese pigs [41]. These findings indicate that pigs can be infected with the 2004 Vietnamese HPAI H5N1 viruses but that these viruses are not readily transmitted between pigs under experimental conditions [41]. In contrast to the above described work, no viral RNA was detected in nasal swabs of pigs infected with avian-derived clade 2.3.4.4 H5Nx viruses in 2014 [31], and only limited detection of viral RNA but failure to isolate infectious virus was reported when pigs were infected with an avian-derived clade 2.3.4.4b H5N1 virus without mammalian-like adaptations [32]. Collectively, these results suggest that some isolates of HPAI H5 subtype viruses can replicate efficiently in the upper respiratory tract of pigs. However, regardless of the presence of infectious virus in nasal and/or oral excretions [31,32,40,41], previous findings indicate a lack of pig-to-pig transmission for H5- or H7-subtype HPAIVs. This is consistent with our findings of the absence of seroconversion in the co-mingled sentinel pigs. Also, the H5N1 clade 2.3.4.4b virus did not transmit to 11 farm workers that had been in close contact with the H5N1-infected minks at the site of the outbreak, indicating a lack of transmission to humans [13]. Furthermore, a recent study showed that two other mink-derived H5N1 viruses which differ by

several amino acids in the PB2, PB1, PA, NA, NS1 and NS2 proteins, did not support transmission to neighboring cages through respiratory droplets in the ferret model [42]. Importantly, it has been previously documented that H5 subtype viruses can acquire the ability to transmit efficiently among pigs through reassortment. Lee *et al.* [43] isolated two H5N2 viruses from pigs showing typical clinical symptoms of influenza-like illness; one was an avian-origin virus, the other one was an avian-swine reassortant virus with PB2, PA, NP and M genes derived from swine influenza viruses. Upon experimental infection of pigs, both viruses could be isolated from nasal swabs, but pig-to-pig transmission occurred only in the group infected with the reassortant H5N2 virus [43].

One of the important findings in this study is that H5N1 viruses inoculated into pigs acquired mammalian-like adaptations, which potentially results in increased fitness of the H5N1 virus in mammalian hosts. There are a total of four mink-derived H5N1 isolates from the infected Spanish farm which were sequenced; all of them possessed the PB2-T271A mutation. The PB2-T271A mutation is known to lead to enhanced polymerase activity in mammalian cells and might contribute to cross-species transmission from avian species to mammals including mink [13,44]. Our results show that the PB2-T271A mutation was stable with no evidence of a change in the frequency of the mutation after replication of the virus for several days in pigs. However, minor variants possessing the mammalian-like E627K mutation in PB2 emerged at low frequencies in this study. The PB2-E627K mutation is a key determinant for mammalian adaptation of avian influenza viruses; its introduction into the genome of an avian IAV enables efficient replication of the avian-origin polymerase complex in mammalian cells; it increases virulence in mice, and contributes to air-borne transmission in ferrets and contact transmission in guinea pigs [45-50]. Similarly, the PB2-E627V substitution was shown to increase viral replication in mammalian cells and virulence in mice models [51]; it was also found in clinical samples in our study as a minor virus population. Furthermore, one oropharyngeal swab possessed a PB2-K526R mutation at the frequency of 3.1%; the K526R mutation was shown to enhance the effect of the PB2-E627K on avian influenza virus replication in mammalian cells and also their virulence in mice [52]. Another key mutation is the HA-Q222L (according to the H5 numbering system) which is equivalent to a Q226L substitution using the H3 numbering system. This mutation was found in one oropharyngeal swab at 1 DPC. Several amino acids in the HA receptor binding site are responsible for switching host specificity; however, the Q222L and G224S substitutions in the

H5 numbering (Q226L and G228S in the H3 numbering) are crucial for increased mammalian-like α 2,6-sialic acid receptor preference in different subtypes of avian IAVs; they are located in the receptor binding domain and interact directly with the host's sialic acid receptor [53]. In addition, the HA-Q222L substitution was previously described to contribute to the emergence of transmissible H5N1 viruses via aerosols after serial passage of H5N1 in ferrets [47,48]. Despite the critical role of these mutations in pathogenicity and transmissibility of IAVs in mammalian hosts, it still remains unclear how the H5N1 clade 2.3.4.4b virus underwent its molecular evolution, and eventually acquired critical mammalian-like adaptations. In addition to the role of pigs in the ecology of IAVs as the “mixing vessel,” the emergence of mammalian-adapted H5N1 viruses in pigs is close to reality; therefore, pigs may serve as the critical target animal to introduce mammalian-like adaptations into avian IAVs although the frequencies of the mammalian-like mutations described here are rather low.

Spillover of H5N1 HPAI clade 2.3.4.4b viruses to mammals and their sustained transmission between mammals has been reported [13,54]. The majority of mammals infected by the HPAI H5N1 clade 2.3.4.4b virus are carnivores, and the consumption of infected dead wild birds is presumably the basis for these spillover events [55]. In contrast to the HPAI H5N1 clade 2.3.4.4b virus infections in wild avians and wild mammals, outbreaks in farmed avian and mammal species pose a much greater risk to humans, due to its close proximity to occupational workers and – in the case of mammalian species – the favorable environment for the acquisition of mammalian-like adaptations. Therefore, evaluating the infectivity/susceptibility and transmissibility of the emerging HPAI viruses in well-established mammalian animal models such as swine and ferrets is crucial to determine their pandemic potential. The present study demonstrated that infection of pigs with the mink-derived clade 2.3.4.4b H5N1 virus led to a productive viral replication in the respiratory tracts of all principal-infected pigs including seroconversion; however, virus shedding from principal-infected pigs was not high and/or frequent enough for an efficient transmission to co-mingled sentinel pigs. Notably, key mammalian-like mutations were found in samples derived from principal-infected pigs. In conclusion, the results obtained in the present study suggest that the mink-derived H5N1 clade 2.3.4.4b virus exhibited increased infectivity in pigs when compared to avian-origin H5N1 clade 2.3.4.4b viruses, however, it did not transmit to co-mingled sentinel animals; therefore, this virus would still be placed in a moderate risk group in terms of transmission ability to humans.

Acknowledgements

We gratefully thank Yonghai Li, Patricia Assato, Michelle Zajac, Isaac Fitz for technical assistance, and Innovative Diagnostics for providing ELISA kits.

Disclosure statement

The J.A.R. laboratory received support from Tonix Pharmaceuticals, Genus plc, Xing Technologies, and Zoetis, outside of the reported work. J.A.R. is inventor on patents and patent applications on the use of antivirals and vaccines for the treatment and prevention of virus infections, owned by Kansas State University. The other authors declare no competing interests.

Funding

Funding for this study was provided through grants from the NIAID supported Center of Excellence for Influenza Research and Response (CEIRR) under contract number 75N93021C00016, the National Bio and Agro-Defense Facility (NBAF) Transition Fund from the State of Kansas, the AMP and MCB Core of the Center on Emerging and Zoonotic Infectious Diseases (CEZID) of the National Institutes of General Medical Sciences under award number P20GM130448, the NIAID Centers of Excellence for Influenza Research and Surveillance (CEIRS) under contract number HHSN 272201400006C and the National Science Foundation (NSF) entitled PIPP Phase I: Next generation surveillance incorporating public health, One Health, and data science to detect emerging pathogens of pandemic potential under award number 2200299.

References

- [1] Tong S, Li Y, Rivaller P, et al. A distinct lineage of influenza A virus from bats. *Proc Natl Acad Sci U S A*. 2012;109(11):4269–4274. DOI:10.1073/pnas.1116200109
- [2] Tong S, Zhu X, Li Y, et al. New world bats harbor diverse influenza A viruses. *PLoS Pathog*. 2013;9(10):e1003657. DOI:10.1371/journal.ppat.1003657
- [3] Vey M, Orlich M, Adler S, et al. Hemagglutinin activation of pathogenic avian influenza viruses of serotype H7 requires the protease recognition motif R-X-K/R-R. *Virology*. 1992;188(1):408–413. DOI:10.1016/0042-6822(92)90775-K
- [4] Xu X, Subbarao, Cox NJ, et al. Genetic characterization of the pathogenic influenza A/Goose/Guangdong/1/96 (H5N1) virus: similarity of its hemagglutinin gene to those of H5N1 viruses from the 1997 outbreaks in Hong Kong. *Virology*. 1999;261(1):15–19. DOI:10.1006/viro.1999.9820
- [5] WHO/OIE/FAO H5N1 Evolution Working Group. Toward a unified nomenclature system for highly pathogenic avian influenza virus (H5N1). *Emerg Infect Dis*. 2008;14(7):e1. DOI:10.3201/eid1407.071681
- [6] World Health Organization. Evolution of the influenza A(H5) haemagglutinin: WHO/OIE/FAO H5 Working Group reports a new clade designated 2.3.4.4 2015. Available from: [https://www.who.int/publications/m/item/evolution-of-the-influenza-a\(h5\)](https://www.who.int/publications/m/item/evolution-of-the-influenza-a(h5))

- haemagglutinin-who-oie-fao-h5-working-group-reports-a-new-clade-designated-2.3.4.4.
- [7] Pohlmann A, King J, Fusaro A, et al. Has epizootic become enzootic? Evidence for a fundamental change in the infection dynamics of highly pathogenic avian influenza in Europe, 2021. *mBio*. 2022;13(4):e0060922.
 - [8] Bevins SN, Shriner SA, Cumbee JC, et al. Intercontinental movement of highly pathogenic avian influenza A(H5N1) clade 2.3.4.4 virus to the United States, 2021. *Emerg Infect Dis*. 2022;28(5):1006–1011. DOI:10.3201/eid2805.220318
 - [9] Shinya K, Ebina M, Yamada S, et al. Influenza virus receptors in the human airway. *Nature*. 2006;440(7083):435–436. DOI:10.1038/440435a
 - [10] World Health Organization. Avian influenza weekly update number. 2023;904.
 - [11] Harfoot R, Webby RJ. H5 influenza, a global update. *J Microbiol*. 2017;55(3):196–203. DOI:10.1007/s12275-017-7062-7
 - [12] World Health Organization. Assessment of risk associated with recent influenza A (H5N1) clade 2.3.4.4b viruses. 2022.
 - [13] Aguero M, Monne I, Sanchez A, et al. Highly pathogenic avian influenza A(H5N1) virus infection in farmed minks, Spain, October 2022. *Euro Surveill*. 2023;28:3. DOI:10.2807/1560-7917.ES.2023.28.3.2300001
 - [14] Ma W, Belisle SE, Mosier D, et al. 2009 pandemic H1N1 influenza virus causes disease and upregulation of genes related to inflammatory and immune responses, cell death, and lipid metabolism in pigs. *J Virol*. 2011;85(22):11626–11637. DOI:10.1128/JVI.05705-11
 - [15] Reed LJ, Muench H. A simple method of estimating fifty per cent endpoints. *Am J Epidemiol*. 1938;27(3):493–497. DOI:10.1093/oxfordjournals.aje.a118408
 - [16] Gaudreault NN, Trujillo JD, Carossino M, et al. SARS-CoV-2 infection, disease and transmission in domestic cats. *Emerg Microbes Infect*. 2020;9(1):2322–2332. DOI:10.1080/22221751.2020.1833687
 - [17] Sponseller BA, Strait E, Jergens A, et al. Influenza A pandemic (H1N1) 2009 virus infection in domestic cat. *Emerg Infect Dis*. 2010;16(3):534–537. DOI:10.3201/eid1603.091737
 - [18] Gauger PC, Vincent AL. Serum virus neutralization assay for detection and quantitation of serum neutralizing antibodies to influenza A virus in swine. *Methods Mol Biol*. 2020;2123:321–333. DOI:10.1007/978-1-0716-0346-8_23
 - [19] Artiaga BL, Morozov I, Ransburgh R, et al. Evaluating alpha-galactosylceramide as an adjuvant for live attenuated influenza vaccines in pigs. *Anim Dis*. 2022;2(1):19. DOI:10.1186/s44149-022-00051-x
 - [20] Lee J, Henningson J, Ma J, et al. Effects of PB1-F2 on the pathogenicity of H1N1 swine influenza virus in mice and pigs. *J Gen Virol*. 2017;98(1):31–42. DOI:10.1099/jgv.0.000695
 - [21] Lee DH. Complete genome sequencing of influenza A viruses using next-generation sequencing. *Methods Mol Biol*. 2020;2123:69–79. DOI:10.1007/978-1-0716-0346-8_6
 - [22] Zhou B, Wentworth DE. Influenza A virus molecular virology techniques. *Methods Mol Biol*. 2012;865:175–192. DOI:10.1007/978-1-61779-621-0_11
 - [23] Hoffmann E, Stech J, Guan Y, et al. Universal primer set for the full-length amplification of all influenza A viruses. *Arch Virol*. 2001;146(12):2275–2289. DOI:10.1007/s007050170002
 - [24] Mena I, Nelson MI, Quezada-Monroy F, et al. Origins of the 2009 H1N1 influenza pandemic in swine in Mexico. *Elife*. 2016;28:5.
 - [25] Joseph U, Su YC, Vijaykrishna D, et al. The ecology and adaptive evolution of influenza A interspecies transmission. *Influenza Other Respir Viruses*. 2017;11(1):74–84. DOI:10.1111/irv.12412
 - [26] Ma W, Vincent AL, Gramer MR, et al. Identification of H2N3 influenza A viruses from swine in the United States. *Proc Natl Acad Sci U S A*. 2007;104(52):20949–20954. DOI:10.1073/pnas.0710286104
 - [27] Garten RJ, Davis CT, Russell CA, et al. Antigenic and genetic characteristics of swine-origin 2009 A(H1N1) influenza viruses circulating in humans. *Science*. 2009;325(5937):197–201. DOI:10.1126/science.1176225
 - [28] World Health Organization. Tool for influenza pandemic risk assessment (TIPRA). 2020.
 - [29] Rajao DS, Vincent AL. Swine as a model for influenza A virus infection and immunity. *ILAR J*. 2015;56(1):44–52. DOI:10.1093/ilar/ilv002
 - [30] Ito T, Couceiro JN, Kelm S, et al. Molecular basis for the generation in pigs of influenza A viruses with pandemic potential. *J Virol*. 1998;72(9):7367–7373. DOI:10.1128/JVI.72.9.7367-7373.1998
 - [31] Kaplan BS, Torchetti MK, Lager KM, et al. Absence of clinical disease and contact transmission of HPAI H5N1 clade 2.3.4.4 from North America in experimentally infected pigs. *Influenza Other Respir Viruses*. 2017;11(5):464–470. DOI:10.1111/irv.12463
 - [32] Graaf A, Piesche R, Sehl-Ewert J, et al. Low susceptibility of pigs against experimental infection with HPAI virus H5N1 clade 2.3.4.4b. *Emerg Infect Dis*. 2023;29(7):1492–1495. DOI:10.3201/eid2907.230296
 - [33] Elsmo EJ, Wunschmann A, Beckmen KB, et al. Highly pathogenic avian influenza A(H5N1) virus clade 2.3.4.4b infections in wild terrestrial mammals, United States, 2022. *Emerg Infect Dis*. 2023;29(12):2451–2460. DOI:10.3201/eid2912.230464
 - [34] Thorsson E, Zohari S, Roos A, et al. Highly pathogenic avian influenza A(H5N1) virus in a harbor porpoise, Sweden. *Emerg Infect Dis*. 2023;29(4):852–855. DOI:10.3201/eid2904.221426
 - [35] Bordes L, Vreman S, Heutink R, et al. Highly pathogenic avian influenza H5N1 virus infections in wild Red foxes (*Vulpes vulpes*) show neurotropism and adaptive virus mutations. *Microbiol Spectr*. 2023;11(1):e0286722. DOI:10.1128/spectrum.02867-22
 - [36] Balzli C, Lager K, Vincent A, et al. Susceptibility of swine to H5 and H7 low pathogenic avian influenza viruses. *Influenza Other Respir Viruses*. 2016;10(4):346–352. DOI:10.1111/irv.12386
 - [37] Richt JA, Lager KM, Janke BH, et al. Pathogenic and antigenic properties of phylogenetically distinct reassortant H3N2 swine influenza viruses cocirculating in the United States. *J Clin Microbiol*. 2003;41(7):3198–3205. DOI:10.1128/JCM.41.7.3198-3205.2003
 - [38] Kida H, Ito T, Yasuda J, et al. Potential for transmission of avian influenza viruses to pigs. *J Gen Virol*. 1994;75(Pt 9):2183–2188. DOI:10.1099/0022-1317-75-9-2183
 - [39] De Vleeschauwer A, Van Poucke S, Braeckmans D, et al. Efficient transmission of swine-adapted but not wholly avian influenza viruses among pigs and from pigs to ferrets. *J Infect Dis*. 2009;200(12):1884–1892. DOI:10.1086/648475
 - [40] Shortridge KF, Zhou NN, Guan Y, et al. Characterization of avian H5N1 influenza viruses

- from poultry in Hong Kong. *Virology*. 1998;252(2):331–342. DOI:10.1006/viro.1998.9488
- [41] Choi YK, Nguyen TD, Ozaki H, et al. Studies of H5N1 influenza virus infection of pigs by using viruses isolated in Vietnam and Thailand in 2004. *J Virol*. 2005;79(16):10821–5. DOI:10.1128/JVI.79.16.10821-10825.2005
- [42] Maemura T, Guan L, Gu C, et al. Characterization of highly pathogenic clade 2.3.4.4b H5N1 mink influenza viruses. *EBioMedicine*. 2023;97:104827. DOI:10.1016/j.ebiom.2023.104827
- [43] Lee JH, Pascua PN, Song MS, et al. Isolation and genetic characterization of H5N2 influenza viruses from pigs in Korea. *J Virol*. 2009;83(9):4205–4215. DOI:10.1128/JVI.02403-08
- [44] Bussey KA, Bousse TL, Desmet EA, et al. PB2 residue 271 plays a key role in enhanced polymerase activity of influenza A viruses in mammalian host cells. *J Virol*. 2010;84(9):4395–4406. DOI:10.1128/JVI.02642-09
- [45] Neumann G, Chen H, Gao GF, et al. H5N1 influenza viruses: outbreaks and biological properties. *Cell Res*. 2010;20(1):51–61. DOI:10.1038/cr.2009.124
- [46] Kim JH, Hatta M, Watanabe S, et al. Role of host-specific amino acids in the pathogenicity of avian H5N1 influenza viruses in mice. *J Gen Virol*. 2010;91(5):1284–1289. DOI:10.1099/vir.0.018143-0
- [47] Herfst S, Schrauwen EJ, Linster M, et al. Airborne transmission of influenza A/H5N1 virus between ferrets. *Science*. 2012;336(6088):1534–1541. DOI:10.1126/science.1213362
- [48] Linster M, van Boheemen S, de Graaf M, et al. Identification, characterization, and natural selection of mutations driving airborne transmission of A/H5N1 virus. *Cell*. 2014;157(2):329–339. DOI:10.1016/j.cell.2014.02.040
- [49] Hatta M, Gao P, Halfmann P, et al. Molecular basis for high virulence of Hong Kong H5N1 influenza A viruses. *Science*. 2001;293(5536):1840–1842. DOI:10.1126/science.1062882
- [50] Steel J, Lowen AC, Mubareka S, et al. Transmission of influenza virus in a mammalian host is increased by PB2 amino acids 627 K or 627E/701N. *PLoS Pathog*. 2009;5(1):e1000252. DOI:10.1371/journal.ppat.1000252
- [51] Taft AS, Ozawa M, Fitch A, et al. Identification of mammalian-adapting mutations in the polymerase complex of an avian H5N1 influenza virus. *Nat Commun*. 2015;6:7491. DOI:10.1038/ncomms8491
- [52] Song W, Wang P, Mok BW, et al. The K526R substitution in viral protein PB2 enhances the effects of E627 K on influenza virus replication. *Nat Commun*. 2014;5:5509. DOI:10.1038/ncomms6509
- [53] Stevens J, Blixt O, Tumpey TM, et al. Structure and receptor specificity of the hemagglutinin from an H5N1 influenza virus. *Science*. 2006;312(5772):404–410. DOI:10.1126/science.1124513
- [54] Lindh E, Lounela H, Ikonen N, et al. Highly pathogenic avian influenza A(H5N1) virus infection on multiple fur farms in the South and Central Ostrobothnia regions of Finland, 2023. *Euro Surveill*. 2023;28:31. DOI:10.2807/1560-7917.ES.2023.28.31.2300400
- [55] Adlhoch C, Fusaro A, Gonzales JL, et al. Avian influenza overview April–June 2023. *EFSA J*. 2023;21(7):e08191.